SCIAMACHY Absorbing Aerosol Index. Calibration issues and global results from 2002 – 2004

M. de Graaf and P. Stammes

Royal Netherlands Meteorological Institute, P.O. Box 201, 3730 AE De Bilt, The Netherlands

Abstract

The Absorbing Aerosol Index (AAI) is the only operational aerosol product from the SCanning Imaging Absorption SpectroMeter for Atmospheric CartograpHY (SCIAMACHY) that has been delivered from the beginning of the measurements of SCIAMACHY. In this paper the validity of the product are discussed. The operational product suffers from calibration errors in the reflectance as measured by SCIAMACHY and design errors. Therefore, a scientific AAI product was constructed, without these errors. Appropriate correction factors were determined for the UV to correct for the radiometric error in the SCIAMACHY reflectances. The algorithm was provided with new LookUp Tables, in which a good representation of polarisation effects was incorporated. The results of this scientific product, from the start of measurements of SCIAMACHY until December 2004, is presented, its validity discussed, and compared to the operational product. The AAI is very sensitive to calibration errors and can be used as a monitor for calibration errors and changes. From 2004 onwards, the SCIAMACHY scientific AAI is suitable to add to the continuation of the long-term AAI record. Recommendations are given for improvement of the operational AAI product.

Correspondence to: M. de Graaf (graafdem@knmi.nl)

1 Introduction

The AAI is an index indicating the presence of ultraviolet (UV)-absorbing aerosols in the Earth's atmosphere. It is derived from the residue, a quantity derived from measured reflectances in the UV (De Graaf et al., 2005). The AAI has been used for a long time in remote sensing to indicate UV-absorbing aerosols, like desert dust and biomass burning aerosols. Initially developed as an error estimate in the Total Ozone Mapping Spectrometer (TOMS) ozone retrieval algorithm (Torres et al., 1998), the residue and AAI records have become the longest records of global aerosol measurements available. Starting with Nimbus–7/TOMS in 1978, American TOMS instruments have provided daily global aerosol maps continuously for over 25 years, with a data gap only between May 1993 and June 1996. From 1995, the European ERS–2/GOME provided additional and independent AAI information, adding to the continuity of the AAI record and validity of the AAI as an aerosol detection quantity (De Graaf et al., 2005). Now, SCIAMACHY will add its independent information to the AAI records, followed in the coming years by OMI/Aura.

Improper characterisation of the instrument's response functions (key data) results at the moment in calibration errors in the measured reflectances of SCIAMACHY of up to 20%. This yields AAI errors in the order of 4-6 (the AAI is dimensionless), which is about 100% of the signal (De Graaf and Stammes, 2002). In this paper, correction factors for the reflectances are used to yield meaningful AAIs and their validity is investigated.

The operational AAI product is calculated using predefined LookUp Tables (LUTs) of theoretical reflectances in a cloud-free and aerosol-free atmosphere. These LUTs were constructed with a radiative transfer model which neglected polarisation effects (Spurr and Balzer, 2000). Here, the AAI is further improved using LUTs in which linear polarisation is accounted for. The effects of this are presented and discussed.

Operational data production of SCIAMACHY started at the end of July 2002. Several improvements and changes of the data processor and key data characteristics followed in the subsequent two and a half years. In this paper the operational AAI product of this period is presented briefly. Additionally, a scientific AAI product, the result of an off-line AAI algorithm using calibrated SCIAMACHY reflectances, off-line LUTs, and additional calibration constants, was determined. These data are presented and investigated, and compared to the operational product and other independent aerosol data.

This paper continues with a brief summary of the theory behind the AAI (section 2). The characteristics of SCIAMACHY are described (section 3), followed by a description of the operational AAI product and its shortcomings (section 3.1). Improvements for an off-line product are discussed, leading to a new algorithm for a scientific AAI (section 3.2), the results of which are laid out in section 4. Finally, the results are discussed and some recommendations for future improvements are given (section 5).

2   Absorbing Aerosol Index

55   The Absorbing Aerosol Index (AAI) separates the spectral contrast, at two wavelengths in the UV, of the atmosphere and a Rayleigh atmosphere caused by aerosol absorption from that of other effects, including molecular Rayleigh scattering, surface reflection, gaseous absorption, and aerosol and cloud scattering. It is derived from the residue.

The residue r is a wavelength-dependent variable that can be defined as (Herman et al., 1997)

$$r_\lambda = -100 \cdot \left\{ {}^{10}\log(\frac{R_\lambda}{R_{\lambda_0}})^{\text{meas}} - {}^{10}\log(\frac{R_\lambda}{R_{\lambda_0}})^{\text{Ray}} \right\}, \tag{1}$$

where R_λ is the reflectance at a wavelength λ. The superscript $^{\text{meas}}$ refers to the measured reflectance in the atmosphere with aerosols, as opposed to a calculated reflectance in an aerosol-free atmosphere with only Rayleigh scattering and absorption by molecules and surface reflection and absorption. The latter is referred to as $^{\text{Ray}}$. The reflectance is defined as $R = \pi I/(\mu_0 E_0)$, where I is the
65   radiance at the top of the atmosphere (TOA), E_0 is the solar irradiance at TOA perpendicular to the direction of the incident sunlight and μ_0 is the cosine of the solar zenith angle θ_0. So $\mu_0 E_0$ is the solar irradiance at TOA incident on a horizontal surface unit.

If the surface albedo A_s for the Rayleigh atmosphere calculation is chosen so that

$$R_{\lambda_0}^{\text{meas}} = R_{\lambda_0}^{\text{Ray}}(A_s), \tag{2}$$

70   where λ_0 is a reference wavelength, equation (1) can be reduced to

$$r_\lambda = -100 \cdot {}^{10}\log(\frac{R_\lambda^{\text{meas}}}{R_\lambda^{\text{Ray}}}), \tag{3}$$

where R_λ^{Ray} is calculated for surface albedo $A_s(\lambda_0)$, so the surface albedo is assumed to be constant in the range $[\lambda, \lambda_0]$. In this paper the traditional residue wavelength pair, $\lambda = 340$ nm and $\lambda_0 = 380$ nm, is adopted. Equation 2 involves an inversion process, which is the core of the residue method
75   algorithm.

Sensitivity studies show (Torres et al., 1998; De Graaf et al., 2005) that UV-absorbing aerosols produce an effect on the spectrum that cannot be simulated with a pure Rayleigh atmosphere and an adjusted surface albedo, creating large, positive residues, even for wavelength independent aerosol refractive indices. Scattering effects are much better represented with a Rayleigh atmosphere and
80   underlying adjusted surface albedo, yielding small, negative residues. The AAI is therefore defined as the positive part of the residue, thereby filtering clouds and scattering aerosols.

3   SCIAMACHY

SCIAMACHY is part of the payload of the European 'Environment Satellite' Envisat, launched on 01 March 2002 onboard an Ariane-5 launch vehicle from the Guyana Space Centre into a polar orbit
85   at about 800 km altitude, with an equator crossing-time of 10:00 AM (local time) for the descending

3

node, orbiting the Earth every 100 minutes. SCIAMACHY is a spectrometer designed to measure sunlight, transmitted, reflected and scattered by the Earth's atmosphere or surface in the ultraviolet, visible and near-infrared wavelength regions (240–2380 nm) at a moderate spectral resolution of 0.2–1.5 nm (Bovensmann et al., 1999). The earthshine radiance is observed in two alternating modes, nadir and limb, yielding data blocks called states. The size of a nadir state is approximately 960×490 km^2. In nadir the Earth is scanned from east to west in four seconds, called a swath, by rotating one of its internal mirrors. The result is a subdivision of the states into groundpixels of approximately 60×30 km^2 at the optical integration time (IT) of 0.25 s. Longer integration times of 0.5 s and 1.0 s also occur, yielding groundpixels of 120×30 km^2 and 240×30 km^2. This is controlled by SCIAMACHY's ground segment, according to its measurement strategy. Even longer integration times occur, but they will not be considered here. The extra-terrestrial solar irradiance is measured each day, once per 14 orbits.

3.1 Operational AAI algorithm

SCIAMACHY's operational AAI product (L2-AAI) is calculated directly after downlinking of the data in the so-called near-realtime level 1 (L1) to level 2 (L2) processing step. The processing steps are described in detail in Balzer et al. (2000). A brief summary is given here, to highlight the most important differences with the scientific AAI product, described below.

The reflectance is determined in the level 0 (L0) to L1 processing step for each groundpixel from channel 2, cluster 9, which contains the spectrum from 320.14 nm to 391.76 nm. Common normal mode ITs in cluster 9 are 0.25 s, 0.5 s and 1.0 s. These are constant within states, but can vary within orbits. The reflectances at 340 nm and 380 nm are used to compute the AAI, using an averaging window, but the width of the window is not given. A Rayleigh reflectance is determined from a predefined LUT, for each pixel, dependent on geometry and surface height. The LUT has inputs for 11 reference heights from 0 to 5 km and 8 reference albedos from 0.0 to 0.9. The geometry is parameterised using polynomial fits. The solar zenith angle θ_0 must be between $15°$ and $85°$ and the viewing zenith angle θ lower than $35°$, otherwise no AAI is calculated.

The L2-AAI suffers from two major flaws. Firstly, the LUTs described above were calculated using the radiative transfer model LIDORT (Spurr et al., 2001). This model neglects polarisation in the Rayleigh scattering calculations. Secondly, the reflectances as measured by SCIAMACHY are underestimated in the UV by 10-20%, as reported by several workers (e.g. Tilstra et al., 2004). This results in an offset of the AAI of about 4-6 (De Graaf et al., 2004), which is of the order of the maximum expected AAI. To correct for these errors, a scientific AAI algorithm was constructed, which uses SCIAMACHY L1 data (calibrated reflectances).

4

3.2   Scientific AAI algorithm

120 The scientific AAI (SC-AAI) is calculated off-line, i.e. after L1 data have been received via satellite link at the Royal Netherlands Meteorological Institute (KNMI). The data are calibrated and radi- ances and irradiances are extracted to determine the reflectances at 340 nm and 380 nm. These reflectances are the normal mean of a one nm wide window. After this, the reflectances are corrected for the underestimation of the reflectance by SCIAMACHY. This correction consists of a simple

125 multiplication of the reflectances by a constant factor. Several factors were tried and the best mul- tiplication factors were 1.210 for R_{340} and 1.130 for R_{380} (Tilstra et al., 2004). Note that different multiplication factors will lead to a linear shift in the resulting AAI (De Graaf et al., 2004, 2005).

The corrected reflectances are used in Equations 2 and 3. The inversion process and the LUTs used therein are described in detail in De Graaf et al. (2005). The LUTs were created using the Doubling-

130 Adding KNMI (DAK) radiative transfer model (De Haan et al., 1987), in which polarisation is accounted for. The surface albedo in Equation 2 is not tabulated, but calculated directly using the assumption of an atmosphere bounded from below by a Lambertian surface (Chandrasekhar, 1960). The surface pressure is corrected for by a second order interpolation.

The changes are illustrated in Figure 1. This figure shows the scientific residue compared to the

135 L2-AAI for 5 states of orbit 10969 on 5 April 2004 over the Sahara, where a dust plume was present at that time. Note that the scientific residue is the quantity that is determined for all SCIAMACHY pixels. The SC-AAI is the quantity that signals the presence of aerosols, or other absorbing effects, by filtering of negative residues. The figure shows the offset of 4-6 of the L2-AAI compared to the scientific residue, caused by the underestimation of the reflectances. Moreover, it shows that

140 the offset is different for east and west pixels, which is caused by the neglect of polarisation in the L2-AAI. This behaviour is found throughout the data.

4   Results

The L2 data can be obtained from the European Space Agency (ESA). The scientific data are avail- able at http://www.temis.nl. Both gridded daily data and gridded monthly means are available as

145 well as daily and monthly pictures. The SC-AAI was determined from all SCIAMACHY L1 data available from 22 July 2002 to 31 December 2004. Some typical examples of results are presented here, highlighting the possibilities and problems of SCIAMACHY AAI data.

The calibration processor of SCIAMACHY has regularly been updated over the last two and half years. This is reflected in the AAI data, which is very sensitive to calibration errors. In that way the

150 AAI can be used as a monitor for calibration errors and improvements. This is illustrated in Figure 2, which shows the number of pixels available at KNMI for the SC-AAI calculation, the processor version number that processed the L1 data of a certain period, and the results. The uppermost panel and the colour code show the L1 processor version number, which reflects the status of the calibration

process. The lower panel shows the number of residues that have been determined in a day. Because all pixels which have a reflectance at 340 nm and 380 nm yield a residue, this is a good measure for the amount of SCIAMACHY data of a certain day available at KNMI.

Processor version number 3.51 was the default when the first data became available. This was steadily updated to version 4.00 in December 2002, but reprocessed data have replaced older versions in this period frequently (the newest available data was always used). From this period not much data was available. In 2003 the processor version was updated from 4.00 to 4.03 and a lot more data became available from December 2002 onwards. In March 2004 the processor version number was updated to 5.01 and from May 2004 onwards often the entire data set was available for processing, although sometimes still entire days were missing.

The centre panel of Figure 2 shows the scientific residue, averaged daily over the globe, as the normal black line and some isolated dots. The bold black line is its 30 day running mean. The daily global scientific residue was highly erratic in the beginning, ranging from -7 and lower to more than 0.5. This is due to the very few number of measurements available at that time and the poor status of the calibration. Often, only one orbit was available on a day and the measurements frequently gave poor results. In 2004 the results improved considerably as the spread in the measurements decreased.

The black diamonds give the monthly mean residues, averaged over the globe. They are not exactly the same as the 30 day running mean, mainly because the monthly means are first monthly averaged per gridbox and then averaged over the globe. In 2004 the monthly mean maps of SC-AAI show very promising results.

The L2-AAI is shown as the purple line. Note that the y-axis is shifted by +6. The L2-AAI correlates well with the scientific residue, although there are clearly differences. In general, the overall pattern is the same and certain peaks coincide. This means that both respond to aerosol events or calibration errors in the reflectances. On the other hand, the differences between the two are the result of the differences of the algorithms, which can be rather profound.

There seems to be some correlation between processor version number and the sign of the differences between the SC-AAI and L2-AAI minus six. For example, the processor version number changes of 4.00 to 4.01, 4.01 to 4.03 and 4.03 to 5.01 seem to coincide with a consistent change in sign between the two. The fact that the difference becomes larger with an upgrade is not necessarily a bad thing; the absolute value of the residue can be shifted quite arbitrarily and the calibration correction of the scientific residue can be chosen so that the value is shifted linearly. It is generally believed that processor versions 5.01 and 5.04 are the best processor versions currently available. With processor version 5.01 and higher the operational product L2-AAI seems to be doing rather well, after correction for the reflectance offset. The problem that remains is the neglect of the polarisation in the Rayleigh atmosphere calculations. This can be solved using improved LUTs.

A typical example of SCIAMACHY SC-AAI measurements is given in Figure 3. This day was chosen because it illustrates a number of specific SCIAMACHY characteristics and problems.

6

Firstly, the daily global coverage of SCIAMACHY is illustrated, which is only $1/6^{\text{th}}$. The black rectangles are the outlines of the nadir states. Only within these states are measurements available. This resolution makes daily monitoring of aerosols difficult, but the data is provided daily to offer the best possible resolution to end-users. Secondly, not all orbits are available, as shown by the irregularly spaced orbits.

This day shows desert dust aerosols over northern Africa, the Middle East region, and parts of China, which are very common in these areas in June. Over the northern Atlantic low SC-AAI values can be observed in a number of states, with clear parts in the east pixels of some states. These are desert dust plumes extending over the Atlantic, with sun glint (see below) pixels removed from the data. Also over the Mediterranean Sea and the northern Pacific some remnants of sun glint can be observed.

Sun glint is a problem that occurred throughout the year. Sun glint is causing a high SC-AAI signal in the eastern pixels of SCIAMACHY. If the sun glint angle is defined as the angle for which sun glint would occur if an ocean was a perfect mirror, the deviation from this angle $\Delta\Omega_{\text{glint}}$ can be defined for each pixel as

$$\cos(\Delta\Omega_{\text{glint}}) = \cos\theta_0 \cos\theta + \sin\theta_0 \sin\theta \cdot \cos(\phi - \phi_0). \tag{4}$$

Because the roughness of the oceans spreads out the sun glint signal, pixels having a sun glint deviation angle $\Delta\Omega_{\text{glint}}$ larger than zero can also be affected by sun glint. The geometrical sun glint condition was defined as the geometry for which the sun glint deviation angle was lower than $12°$. A pixel satisfied the sun glint condition when it satisfied the geometrical sun glint condition and had an ocean as underlying surface. The underlying surface was determined using the $0.25°\times0.25°$ GTOPO elevation database with an ocean flag. Pixels satisfying the sun glint condition were removed.

The residues of all pixels satisfying the sun glint condition of three months (October – December 2004) were compared to all land pixels satisfying the geometrical sun glint condition. The average residue of the sun glint pixels was -0.38 and that of the land pixels was -1.38. The average residue for pixels not satisfying the geometrical sun glint condition was -1.56 over both land and ocean. This was considered a confirmation that the high residue in ocean sun glint pixels was anomalous and caused by sun glint.

The effect of using a sun glint deviation angle $\Delta\Omega_{\text{glint}}$ lower than $12°$ is illustrated in Figure 4. Figure 4a shows the sun glint deviation angle for SCIAMACHY pixels on 12 December 2004 over the Indian Ocean, Indonesia and Australia, and the south–west Pacific. The pixels satisfying the sun glint condition are marked in red, other ocean pixels' sun glint deviation angles are marked according to the continuous colour scale. Figure 4b shows the SC-AAI when no sun glint mask is applied. Several bands with high SC-AAI values can be distinguished in the eastern pixels over the oceans, but not over land. Applying the $12°$ sun glint deviation angle mask removes most of the pixels with high signals (Figure 4c). A more severe sun glint mask, e.g. removing all ocean pixels with sun glint deviation angles lower than $15°$, improves the picture on 12 December 2004, because

7

it is not likely that any aerosol events caused the high signals on this day in the area shown. But the sun glint mask does not discriminate between sun glint and aerosol events and for situations with aerosol plumes over the oceans, the sun glint mask will remove pixels with aerosol information. To reduce this problem the condition was set strict enough that sun glint is removed from most of the pixels, leaving only some small remnants in clear sky pixels with sun glint deviation angles close to $12°$. These remnants will not easily be mistaken for artificial aerosol events. On the other hand, the condition is not so strict that it will remove all aerosol pixels from aerosol plumes over oceans. The location of pixels satisfying the sun glint condition are easily recognised and the gaps which the sun glint mask produces are small enough so they will not greatly reduce the signal caused by aerosols.

In Figure 5 three-monthly means of 2004 are presented to show the most persistent aerosol sources and seasonal variations. The range of the AAI data plotted in Figure 5 is from -0.4 to 2.5. Theoretically, a well-calibrated AAI should range from zero up to indicate absorbing aerosols. In reality some fine-tuning is needed to establish the right threshold. Figure 2 shows that the average of the scientific residue is about -2, lower than the global average GOME residue in the period 1995 – 2000 (De Graaf et al., 2005), which was -1.2. The correction factors for the SCIAMACHY reflectance offset are probably too severe, causing the residue to be smaller than usual. Therefore, the lower plotting boundary was lowered to -0.4.

The first panel of Figure 5 is the average of the monthly means of January, February and December of 2004. Only a few persistent aerosol sources over the Sahara show up in the plot. As was shown in Figure 2, the average AAI in the first two months of 2004 was very low, probably due to incorrect calibration. Still, the southern part of the Sahara shows some signal.

The next panel in Figure 5 shows the boreal spring main aerosol sources. As was found with GOME (De Graaf et al., 2005), very persistent aerosol sources are found over northern Africa and the Middle East. SCIAMACHY also detects the aerosol plumes north-west of India, which were never detected by GOME because of its data storage problem in that region.

In the summer the typical desert dust plume over the Sahara, extending far over the northern Atlantic, is clearly present. This is one of the most prominent features of the AAI and can be observed in all summer months. Also the biomass burning aerosol plume west of Angola, that was found every summer of 1995 – 2000 by GOME, is present. The aerosol plumes over the northern Sahara and the Middle East are strongest and most persistent, as a result of the most northerly position of the Inter-Tropical Convergence Zone (ITCZ) at that moment.

In autumn all aerosol plumes present in the summer are weaker, but still discernible. A clear plume is visible over the north-west of Australia. This plume frequently showed up in the GOME data as well, but was difficult to distinguish from the noise, because of the large footprint of GOME (40×320 km^2). SCIAMACHY data however, clearly shows a persistent aerosol source in this area. Possible sources might be desert dust from Australia or biomass burning from Indonesia and Australia or both.

265   The SCIAMACHY AAI values were also compared to the TOMS AAI (Figure 6). This figure shows the zonally averaged SC-AAI in 2002, 2003 and 2004, for SCIAMACHY between 60°S and 60°N. Note that the TOMS scale is differents from the scale of SCIAMACHY. The definition of the TOMS AAI has changed with the introduction of version 8 data (2004), which has increased the sensitivity of the TOMS index. In this figure the AAIs were averaged, not the residues, which

270   means that only positive values are considered. So TOMS' higher sensitivity and greater daily global coverage creates much higher zonal means. A comparison of residues would make more sense, but TOMS residues are no longer available. So only a qualitative comparison is possible. The different scale is, however, also an indication that SCIAMACHY values are lower than expected.

Figure 6 shows that SCIAMACHY performs badly in 2002, no clear zonal pattern is discernible in

275   this year. In 2003 a local peak is seen around 25° N, but the picture is mostly determined by the noise near the poles. The SCIAMACHY AAI is cut-off above 60°N and S, but even before that the noise level exceeds the signal. In 2004 the noise level has dropped below the signal level and is confined to a region near 60°N and S. A clear peak in the AAI can be distinguished between 5° − 30°N, which is where the major Northern Hemisphere (NH) deserts are located. A smaller peak can be found on

280   the Southern Hemisphere (SH), between 0° − 30°S. This behaviour is also found in TOMS AAI, although the relative differences between the NH and SH are less than in the SC-AAI. In the period 1996 – 2000 both TOMS and GOME found a similar behaviour, with a large difference between the NH and SH (De Graaf et al., 2005).

5   Conclusions

285   The scientific Absorbing Aerosol Index product (SC-AAI) of SCIAMACHY shows promising results. The underestimated reflectance of SCIAMACHY in the UV (Tilstra et al., 2004) was corrected with constant multiplication factors at the AAI wavelengths 340 nm (1.210) and 380 nm (1.130). This resulted in an AAI that is almost in the expected range of lower than zero for scattering events (clouds and scattering aerosols) and higher than zero for absorbing aerosols. However, Figures 5

290   and 6 show that some fine tuning is still necessary. Better calibration of the reflectances might improve this feature.

The SC-AAI algorithm accounts for polarisation in the Rayleigh reflectances, thereby improving the viewing angle offset found in the operational AAI product (L2-AAI). As the L2-AAI is calculated in the level 1 to level 2 processing stage, the LUTs used by the processor can easily be updated using

295   a radiative transfer model incorporating (linear) polarisation. This would improve the L2-AAI and make it a useful product. The only problem remaining then for the operational product would be the reflectance offset, which can be corrected using a linear shift of the AAI. This change of LUTs is highly recommended.

The SCIAMACHY SC-AAI has reveiled sun glint related problems in the interpretation of the

9

300   AAI. Sun glint can easily be defined geometrically, but the sun glint mask used for SCIAMACHY pixels does not distinguish between high AAIs as a result from sun glint or from aerosol events. This might be improved using the absolute value of the reflectances. Absorbing aerosol events reduce the reflectances, but more so at the lower wavelength, causing a positive residue. It is anticipated that sun glint will increase the reflectances, but probably more so at the higher wavelength, also creating

305   a positive residue.

    The SC-AAI in 2004 gives good results, especially after March 2004, when the processor version was updated to version 5.01. The seasonal means in 2004 show the same characteristics as were found by GOME in 1995 – 2000 and the same as found by TOMS. This makes SCIAMACHY suitable for the continuation of the long-term AAI record, now that GOME is failing and EP/TOMS

310   is suffering from degradation.

References

Balzer, W., Spurr, R., Thomas, W., Kretschel, K., and Bollner, M.: SCIAMACHY level 1b to 2 NRT Processing Input/Output Date Definition, Tech. Rep. ENV-TN-DLR-SCIA-0010, Issue 3/B, Dtsch. Zent. für Luft- und Raumfahrt, Oberpfaffenhofen, Germany, 2000.

Bovensmann, H., Burrows, J. P., Buchwitz, M., Frerick, J., Noël, S., Rozanov, V. V., Chance, K. V., and Goede, A. P. H.: SCIAMACHY: Mission Objectives and Measurement Modes, J. Atmos. Sci., 56, 127–150, 1999.

Chandrasekhar, S.: Radiative Transfer, Dover, Mineola, N.Y., 1960.

De Graaf, M. and Stammes, P.: First verification of SCIAMACHY's Absorbing Aerosol Index product, in Envisat Calibration Review Proceedings, ESA Special publication SP-531, 2002.

De Graaf, M., Tilstra, L. G., and Stammes, P.: SCIAMACHY absorbing aerosol index: the scientific product compared to the operational product and TOMS data, in Envisat Calibration Review Proceedings, ESA Special publication SP-562, 2004.

De Graaf, M., Stammes, P., Torres, O., and Koelemeijer, R. B. A.: Absorbing Aerosol Index: Sensitivity Analysis, application to GOME and comparison with TOMS, J. Geophys. Res., 110, 2005.

De Haan, J. F., Bosma, P. B., and Hovenier, J. W.: The adding method for multiple scattering calculations of polarized light, Astron. Astr., 183, 371–391, 1987.

Herman, J. R., Bhartia, P. K., Torres, O., Hsu, C., Seftor, C., and Celarier, E. A.: Global distributions of UV-absorbing aerosols from NIMBUS 7/TOMS data, J. Geophys. Res., 102, 16,911–16,922, 1997.

Spurr, R. and Balzer, W.: SCIAMACHY level 1c to 2 Off-line Processing. Algorithm Theoretical Basis Document, Tech. Rep. ENV-ATB-SAO-SCI-2200-0003, Issue 2, Dtsch. Zent. für Luft- und Raumfahrt, Oberpfaffenhofen, Germany, 2000.

Spurr, R. J. D., Kurosu, T. P., and Chance, K. V.: A Linearized discrete Ordinate Radiative Transfer Model for Atmospheric Remote Sensing Retrieval, J. Quant. Spectrosc. Radiat. Transfer, 68, 689–735, 2001.

Tilstra, L., van Soest, G., de Graaf, M., Acarreta, J., and Stammes, P.: Reflectance comparison between SCIAMACHY and a radiative transfer code in the UV, in Proceedings of the Second Workshop on the Atmospheric Chemistry Validation of ENVISAT (ACVE-2), ESA Special publication SP-562, 2004.

Torres, O., Bhartia, P. K., Herman, J. R., Ahmad, Z., and Gleason, J.: Derivation of aerosol properties from satellite measurements of backscattered ultraviolet radiation: Theoretical basis, J. Geophys. Res., 103, 17,099–17,110, 1998.

Figure Captions

Fig. 1. The scientific residue compared to the operational level-2 AAI data for orbit 10969, states 5–9. The colours refer to pixels with approximately the same viewing geometry. The first four pixels of 30×60 km^2 in a forward swath are called East pixels, the next 4 Centre–east, the next 4 Centre–west and the last 4 West pixels.

Fig. 2. Statistics of the off-line data as a function of time for the entire measurement period, 22 July 2002 – 31 December 2004. The uppermost panel and the colour codes denote the L1 processor version number of the data of a certain period. The central panel shows the data, averaged per day over the entire globe. The normal black line and individual points show the daily global averaged scientific residue. The bold black line is its 30 day running mean. The black diamonds show the monthly mean scientific residue. The purple line shows the L2-AAI (Note that the right axis is shifted by +6). The lower panel shows the number of pixels that where available for the scientific residue calculations per day.
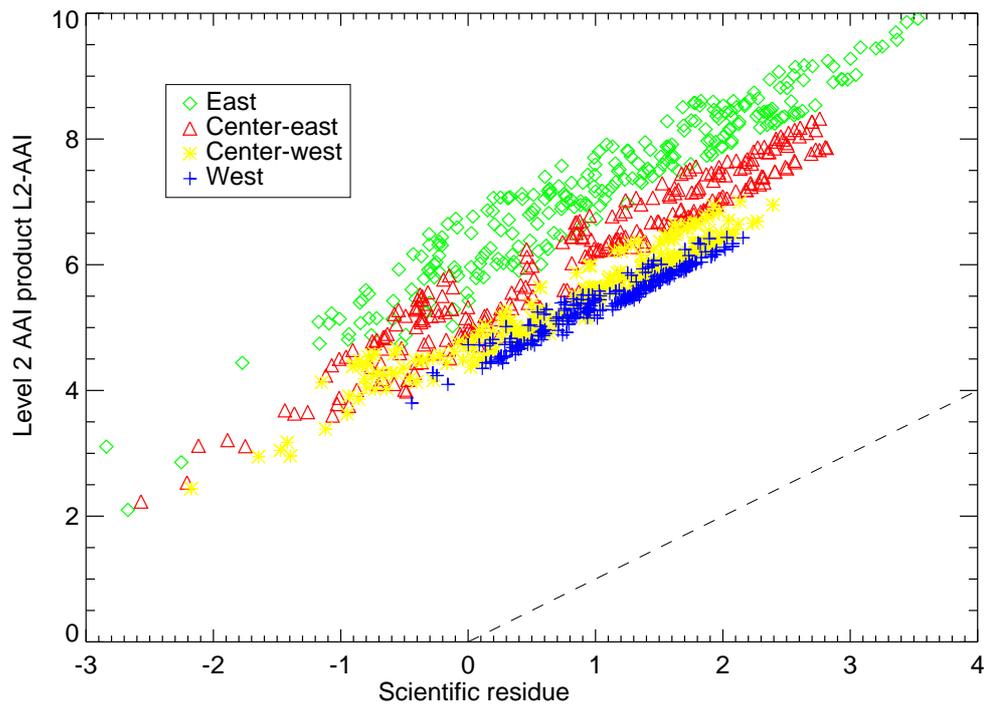
Fig. 3. Global SCIAMACHY SC-AAI on 16 June 2004. The black rectangles are the outline of the nadir states.

Fig. 4. SCIAMACHY SC-AAI on 12 December 2004 over the Indian Ocean, Indonesia and Australia, and the south-western Pacific. a) Sun glint deviation angle of SCIAMACHY ocean pixels. The sun glint deviation angle has a smooth scale, but all pixels satisfying the sun glint condition, i.e. having a sun glint deviation angle lower than $12°$, are marked in red. b) SC-AAI without sun glint mask. c) SC-AAI with all ocean pixels with a sun glint deviation angle lower than $12°$ removed.
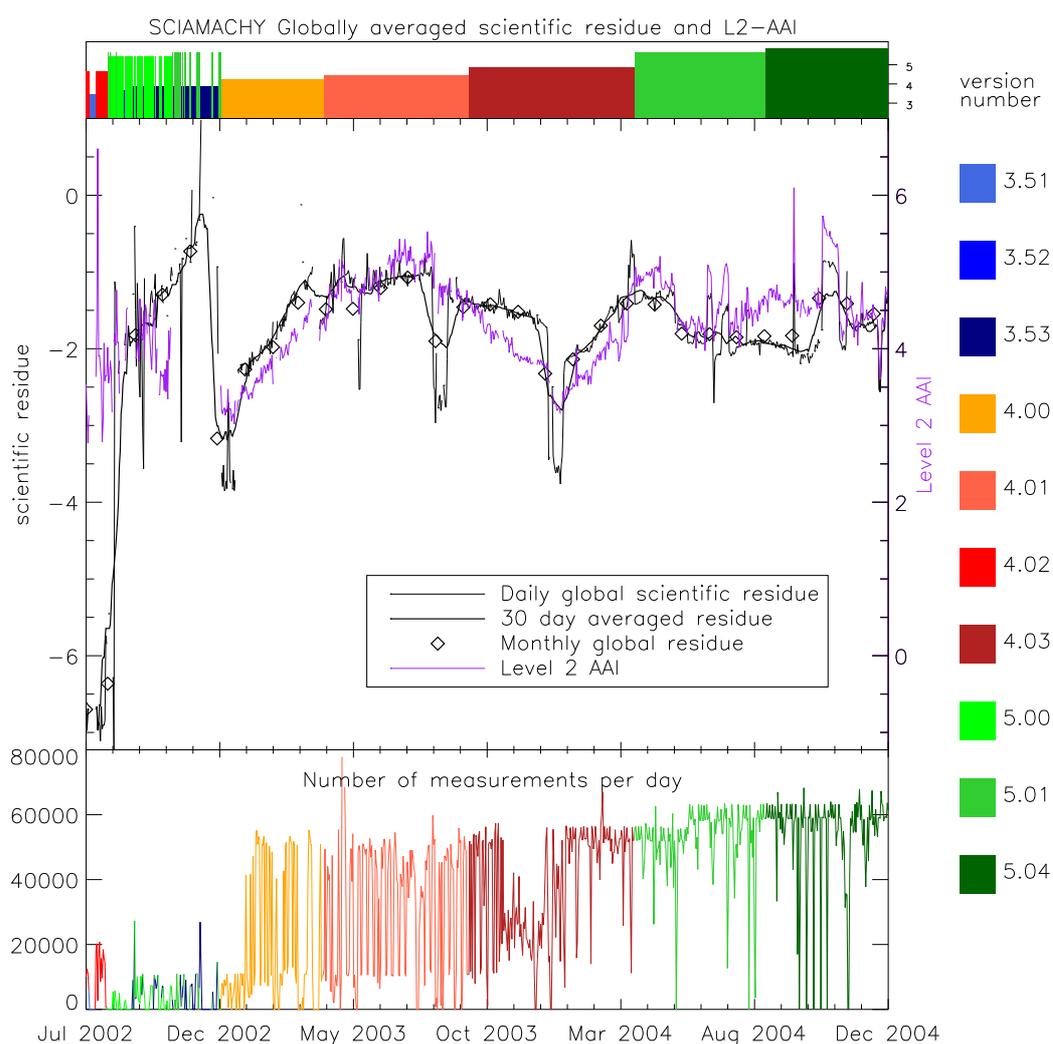
Fig. 5. Maps of the seasonally averaged global SC-AAI. Shown are the mean SC-AAI in January, February and December of 2004 (Winter), mean SC-AAI in March, April and May 2004 (Spring), mean SC-AAI in June, July and August 2004 (Summer) and mean SC-AAI in September, October and November 2004 (Autumn).

Fig. 6. Zonal mean SC-AAI from SCIAMACHY (solid line) and TOMS (dashed-dotted line) in 2002, 2003 and 2004.
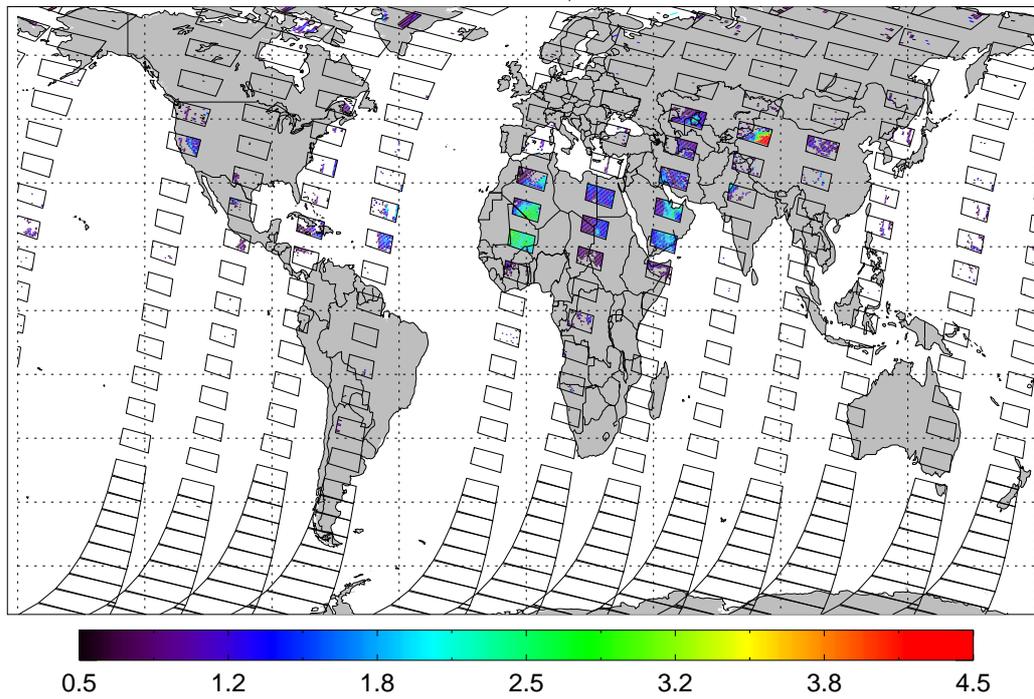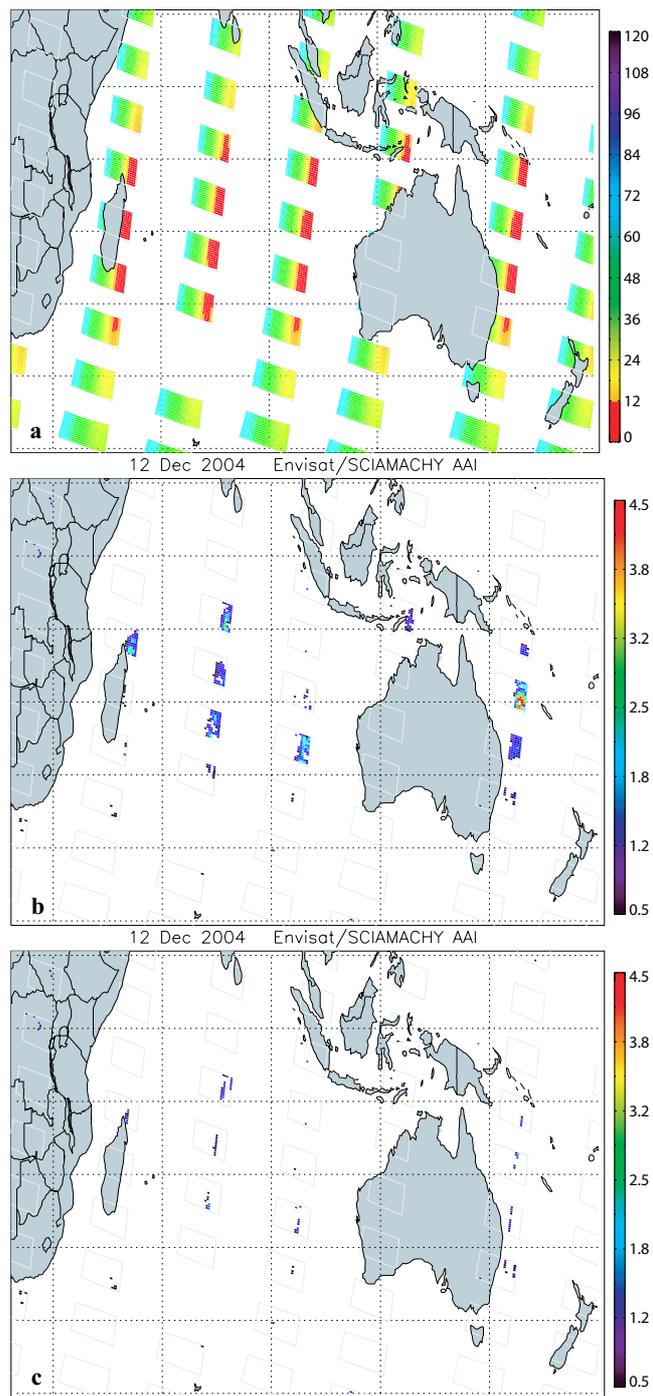
Fig. 1. The scientific residue compared to the operational level-2 AAI data for orbit 10969, states 5–9. The colours refer to pixels with approximately the same viewing geometry. The first four pixels of 30×60 km^2 in a forward swath are called East pixels, the next 4 Centre–east, the next 4 Centre–west and the last 4 West pixels.

13

Fig. 2. Statistics of the off-line data as a function of time for the entire measurement period, 22 July 2002 – 31 December 2004. The uppermost panel and the colour codes denote the L1 processor version number of the data of a certain period. The central panel shows the data, averaged per day over the entire globe. The normal black line and individual points show the daily global averaged scientific residue. The bold black line is its 30 day running mean. The black diamonds show the monthly mean scientific residue. The purple line shows the L2-AAI (Note that the right axis is shifted by +6). The lower panel shows the number of pixels that where available for the scientific residue calculations per day.
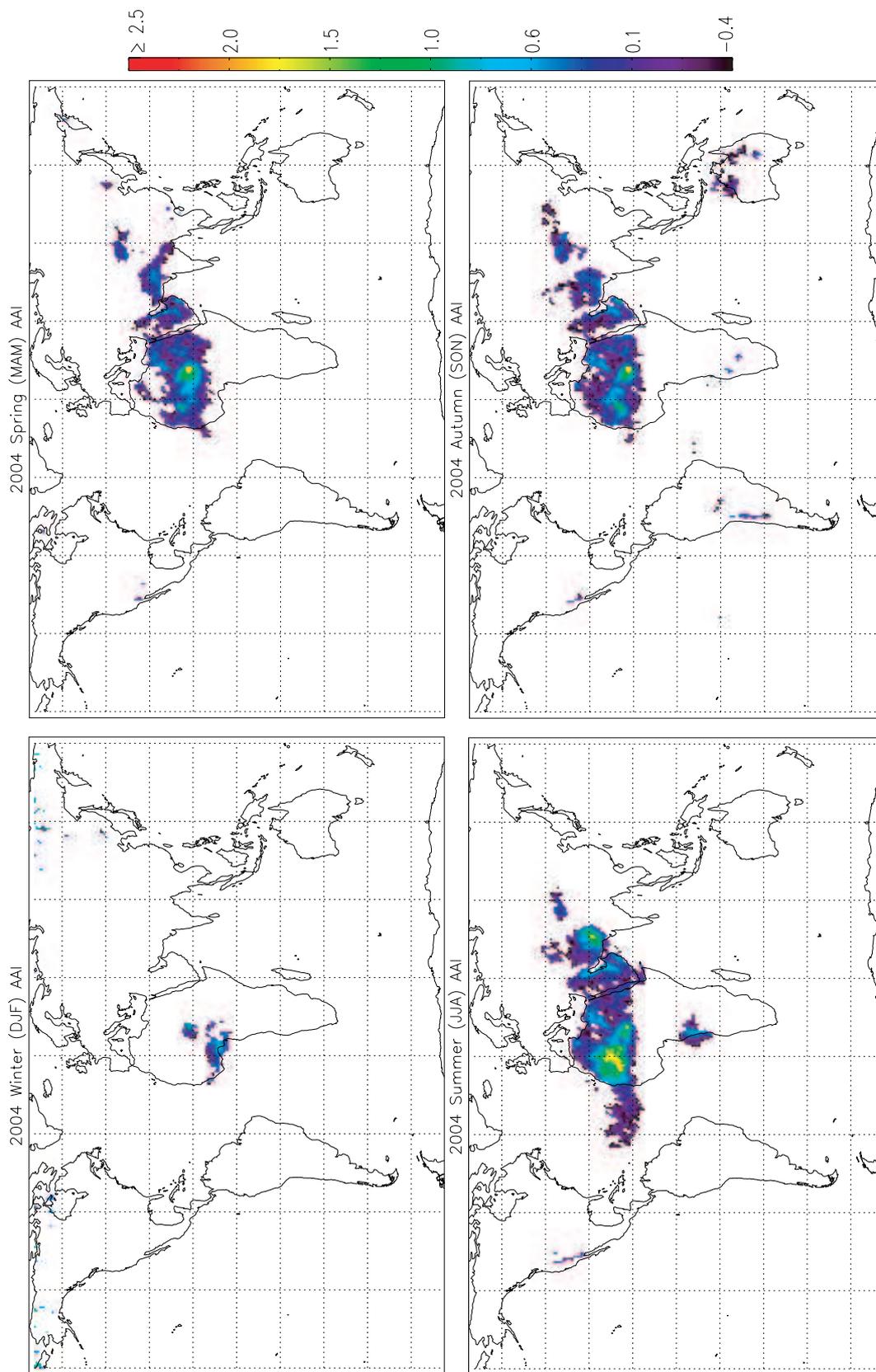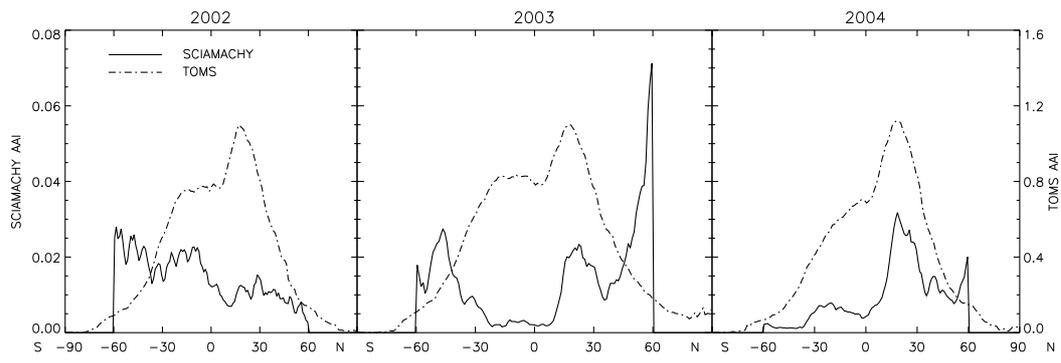
Fig. 3. Global SCIAMACHY SC-AAI on 16 June 2004. The black rectangles are the outline of the nadir states.

Fig. 4. SCIAMACHY SC-AAI on 12 December 2004 over the Indian Ocean, Indonesia and Australia, and the south-western Pacific. a) Sun glint deviation angle of SCIAMACHY ocean pixels. The sun glint deviation angle has a smooth scale, but all pixels satisfying the sun glint condition, i.e. having a sun glint deviation angle lower than 12°, are marked in red. b) SC-AAI without sun glint mask. c) SC-AAI with all ocean pixels with a sun glint deviation angle lower than 12° removed.

16

Fig. 5. Maps of the seasonally averaged global SC-AAI. Shown are the mean SC-AAI in January, February and December of 2004 (Winter), mean SC-AAI in March, April and May 2004 (Spring), mean SC-AAI in June, July and August 2004 (Summer) and mean SC-AAI in September, October and November 2004 (Autumn).

Fig. 6. Zonal mean SC-AAI from SCIAMACHY (solid line) and TOMS (dashed-dotted line) in 2002, 2003 and 2004.